Title

Comparative transcriptome analysis by deep RNA sequencing at early stage of skin pigmentation in goats (*Capra hircus*)

Authors

Hangxing Ren[*,†,1], Gaofu Wang[*,†,1], Jing Jiang[*,†], Liangjia Liu[*,†], Nianfu Li[‡], Jie Li[*,†], Lin Fu[*,†], Haiyan Zhang[‡], Risu Na[§], Yongfu Huang[§], Li Zhang [*], Lei Chen[*], Yong Huang[*,2], and Peng Zhou[*,†,2]

Affiliation

[*] Chongqing Academy of Animal Sciences, Chongqing, 402460,China

[†] Chongqing Engineering Research Center for Goats, Chongqing, 402460, China

[‡]Youyang Animal Husbandry Bureau, Chongqing, 409800, China

[§] Department of Animal Science, Southwest University, Chongqing, 400715, China

[1] The authors contribute equally to this work

[2] Corresponding author

Running title

Dermal hyperpigmentation in goat

Key words

dermal pigmentation; transcriptome; melanin; goat

Corresponding author

Yong Huang, Changlong Street 51#, Rongchang District, Chongqing, China 406420; Tel: +86-023-46792355; huangyongcqbb@126.com

Peng Zhou, Changlong Street 51#, Rongchang District, Chongqing, China 406420; Tel: +86-023-46792015; cqzp2006@163.com

ABSTRACT

Although specific genes have been found to be associated with skin pigmentation, the global gene expression profile for the early stage of skin pigmentation and development in mammals is still not well understood. Here we reported a rare natural group of goat (Youzhou dark goat) featuring the dark skin of body including the visible mucous membranes, which may be an exclusive kind of large mammalian species with this special phenotype so far. In the present study, we characterized the 100-day-old fetal skin transcriptome in hyperpigmented (dark-skinned) and wild-type (white-skinned) goats using deep RNA-sequencing. A total of 923,013,870 raw reads from 6 libraries were obtained, and a large number of alternative splicing events were identified in the transcriptome of fetal skin, including the well-known melanogenic genes *ASIP*, *TYRP1*, and *DCT*, which were differentially expressed in the skin between the dark-skinned and white-skinned goats. Further analysis demonstrated that differential genes including *ASIP*, *TYRP1*, *DCT*, *WNT2*, *RAB27A*, *FZD4*, and *CREB3L1* were significantly overrepresented in the *melanogenesis* pathway and several biological process associated with pigmentation. On the other hand, we identified 1616 novel transcripts in goat skin based on the characteristics of their expression level and gene composition. These novel transcripts may represent two distinct groups of nucleic acid molecules. Our findings contribute to the understanding of the characteristics of global gene expression at early stages of skin pigmentation and development, as well as describe an animal model for human diseases associated with pigmentation.

INTRODUCTION

Skin pigmentation is a complex process that includes melanin biosynthesis in melanocytes, which

is transferred to keratinocytes (Wolff 1973; Seiberg 2001). Unlike the numerous variations of coat color, there are only a few natural variants of skin color in other mammals compared to the phenotypes of human skin color. As a result, most studies on the genetics of skin pigmentation are conducted in humans (Baxter and Pavan ; Sturm 2009; Quillen and Shriver 2011; Meng *et al.* 2012) and mice (Bennett and Lamoreux 2003; Garcia *et al.* 2008), in which 378 color genes (171 cloned genes and 207 uncloned genes) have been identified (http://www.espcr.org/micemut) to date. However, only a small portion of these color genes have been identified as candidate causative genes for skin pigmentation in different populations of humans, mice/rats, and sheep, including *ASIP*, *TYRP1*, *DCT*, *TYR*, *HERC2*, *OCA2*, *MC1R*, *SLC24A5*, *SLC45A2*, *IRF4*, *KITLG* (Slominski *et al.* 2004; Yamaguchi *et al.* 2007; Ebanks *et al.* 2009; Yamaguchi and Hearing 2009; Garcia-Gamez *et al.* 2011; Kondo and Hearing 2011; Liu *et al.* 2013; Raadsma *et al.* 2013; Han *et al.* 2015). In addition, few studies have characterized the global gene expression profile of skin pigmentation and development. Although investigations of the skin transcriptome have recently been conducted on coat color (Fan *et al.* 2013) and hair follicles (Xu *et al.* 2013a; Xu *et al.* 2013b; Wang *et al.* 2015; Yue *et al.* 2015; Gao *et al.* 2016) in sheep and goats, and skin color in the common carp (Jiang and Bikle 2014b; Wang *et al.* 2014), red tilapia (Zhu *et al.* 2016), and chickens (Zhang *et al.* 2015), the genetic basis for skin pigmentation is not well understood compared to that of hair or coat color.

Here, we report a rare indigenous goat breed (Youzhou dark goat) that features dark skin of the body including the visible mucous membranes (Fig.1A), which is a rare fibromelanosis that has previously only been reported in the Silky fowl (Nozaki and Makita 1998; Muroya *et al.* 2000; Dorshorst *et al.* 2011; Shinomiya *et al.* 2012). The pigmentation phenotype of the Youzhou dark goat significantly differs from the piebald phenotype of the bovine (Weikard *et al.* 2013),

whereas it is similar to a recently reported case of dermal melanocytosis in humans (Lee *et al.* 2010). However, the underlying mechanism of this hyperpigmentation is yet to be explored. Therefore, the Youzhou dark goat can be used as a medical model to study human diseases associated with pigmentation, such as skin melanopathy, melanosis coli, and mucosal melanosis. Interestingly, based on our long-term observations (unpublished), skin pigmentation parallels skin development during the pregnant and postnatal period in the Youzhou dark goat. Consequently, to understand fibromelanosis in mammals, it is necessary to investigate the biology of skin pigmentation at early developmental stages in goats. In developmental embryology, the growth of the fetal skin peaks at approximately 100 days of gestation in sheep and goats (Wang *et al.* 1996; Qin 2001). In the present study, we used the Youzhou dark goat (hyperpigmented or dark-skinned) and Yudong white goat (wild-type or white-skinned) as models of skin pigmentation to characterize the skin transcriptome in 100-day-old fetal goats using deep RNA-sequencing. Our study not only contributes to the understanding of the biology of skin pigmentation and development but also provides valuable information towards understanding human melanocytosis.

MATERIALS AND METHODS

Ethical statement

All surgical procedures in goats were performed according to the Regulations for the Administration of Affairs Concerning Experimental Animals (Ministry of Science and Technology, China; revised in June 2004) and adhered to the Reporting Guidelines for Randomized Controlled Trials in Livestock and Food Safety (REFLECT).

Animals

Two goat groups with different skin pigmentation phenotypes were investigated in this study. The Yudong white goat (*Capra hircus*) is distributed in Southwest China (located at 31°14'-32°12' N and 108°15'-109°58' E) and features white color in the coat and skin. The Youzhou dark goat (*Capra hircus*) is an indigenous breed uniquely distributed in Youyang County in Chongqing, China (located at 26°54' N and 108°57' E) and features dark skin of the body including the visible mucous membranes but a generally white coat color. Briefly, three pregnant ewes from each breed were subjected to a caesarean section to collect the fetuses (n=3) at 100 days of gestation, and then the dorsal and ventral skins were collected from each fetus. The first sample (3 grams) was dissected and rapidly frozen whole in isopentane chilled over liquid nitrogen for histological examination. The second sample (3 grams) was snap-frozen in liquid nitrogen for RNA-sequencing and qPCR analysis.

RNA isolation, library preparation and sequencing

In the present study, a total of 6 libraries were generated for sequencing according to the sample size (n=6) in two breeds of goats. For each of the 6 fetal goats, total RNA was isolated using TRIzol reagent (Invitrogen, USA) according to the manufacturer's instructions. RNA degradation and contamination was monitored on 1% agarose gels. RNA purity was checked using the NanoPhotometer spectrophotometer (Implen, USA). RNA concentration was measured using a Qubit RNA Assay Kit with a Qubit 2.0 Flurometer (Life Technologies, USA). RNA integrity was assessed using the RNA Nano 6000 Assay Kit with the Agilent 2100 Bioanalyzer System (Agilent Technologies, USA). A total of 3 μg of RNA per sample was used as the input material for the RNA sample preparations. First, ribosomal RNA was removed using the Epicentre Ribo-zero™ rRNA Removal Kit (Epicentre, USA), and rRNA free residue was cleaned up using ethanol precipitation. Subsequently, the highly strand-specific libraries were generated using the

rRNA-depleted RNA using the NEBNext Ultra™ Directional RNA Library Prep Kit for Illumina (NEB, USA) according to the manufacturer's recommendations. Briefly, fragmentation was carried out using divalent cations under elevated temperature in NEBNext. First strand cDNA was synthesized using random hexamer primers and M-MuLV Reverse Transcriptase (RNaseH-). Second strand cDNA synthesis was subsequently performed using DNA Polymerase I and RNase H. In the reaction buffer, dNTPs with dTTP were replaced by dUTP. The remaining overhangs were converted into blunt ends via exonuclease/polymerase activities. After adenylation of the 3' ends of the DNA fragments, NEBNext Adaptor with hairpin loop structure were ligated to prepare for hybridization. To select cDNA fragments of preferentially 150-200 bp in length, the library fragments were purified using the AMPure XP system (Beckman Coulter, USA). Then, 3 μl of USER Enzyme (NEB, USA) was used with size-selected, adaptor-ligated cDNA at 37°C for 15 min followed by 5 min at 95°C before PCR. PCR was performed with Phusion High-Fidelity DNA polymerase, Universal PCR primers and Index (X) Primer. Finally, the products were purified (AMPure XP system) and the library quality was assessed on the Agilent 2100 Bioanalyzer System. The clustering of the index-coded samples was performed on a cBot Cluster Generation System using TruSeq PE Cluster Kit v3-cBot-HS (Illumina) according to the manufacturer's instructions. After cluster generation, the libraries were sequenced on an Illumina Hiseq 2000 platform and 100 bp paired-end reads were generated.

Quality control

The raw data were firstly processed through in-house perl scripts. In this step, clean data were obtained by removing the reads containing adapters, reads containing over 10% of ploy-N sequences, and low quality reads (more than 50% of bases with Phred scores less than 5%) from the raw data. The Phred score (Q20, Q30) and GC content of the clean data were calculated. All

the subsequent analyses were based on the high quality data. The sequencing data were submitted to the Genome Expression Omnibus (Accession Numbers GSE69812) in NCBI.

Mapping to the reference genome

The reference genome and gene model annotation files were downloaded directly from the genome website (http://goat.kiz.ac.cn). The index of the reference genome was built using Bowtie v2.0.6 (Langmead *et al.* 2009; Langmead and Salzberg 2012) and paired-end clean reads were aligned to the reference genome using TopHat v2.0.9 (Trapnell *et al.* 2012; Kim *et al.* 2013).

Transcriptome assembly

The goat reference genome and gene model annotation files were downloaded directly from the genome website (http://goat.kiz.ac.cn). The index of the reference genome was built using Bowtie v2.0.6 (Langmead *et al.* 2009; Langmead and Salzberg 2012) and paired-end clean reads were aligned to the reference genome using TopHat v2.0.9 (Trapnell *et al.* 2012; Kim *et al.* 2013). The mapped reads of each sample were assembled using both Scripture (beta2) (Guttman *et al.* 2010) and Cufflinks (v2.1.1) (Trapnell *et al.* 2010) in a reference-based approach. Scripture was run with default parameters. Cufflinks was run with 'min-frags-per-transfrag=0' and '--library-type fr-firststrand', with all other parameters set as default.

Quantification of gene expression level

Cuffdiff (v2.1.1) was used to calculate the FPKM (fragments per kb for a million reads) of both lncRNAs and coding genes in each sample (Trapnell *et al.* 2010). For biological replicates (n=3), transcripts or genes with a *P*-adjust<0.05 were considered differentially expressed between the two groups of goats (dark-skinned and white-skinned).

Alternative splicing analysis

Alternative splicing (AS) events were classified into 12 basic types using the software Asprofile v1.0 (Florea *et al.* 2013). The number of AS events in each of the 6 samples was estimated separately. We used DEXSeq software(Anders *et al.* 2012) for the differential exon usage analysis of the AS transcripts, in which a general linear model was employed for the differential analysis of exon expression and a *P*-adjust<0.05 indicated a significant result.

Identification of novel transcripts

To identify the novel transcripts from clean data, we first distinguished the novel transcripts and the candidate long noncoding RNAs using four tools including CNCI (v2) (Sun *et al.* 2013), CPC (0.9-r2) (Kong *et al.* 2007), Pfam-scan (v1.3) (Punta *et al.* 2012), and PhyloCSF (v20121028) (Lin *et al.* 2011). Transcripts predicted to be without coding potential by all of four tools above were filtered away (which are considered as the candidate long noncoding RNAs), and those with coding potential (which are selected by either of four tools above) but lacking of any known annotation were kept and considered as the novel transcripts in the present analysis. Quantification of gene expression level were estimated by calculating FPKMs of the novel transcripts.

RepeatMasker (http://www.repeatmasker.org/cgi-bin/WEB RepeatMasker) was used with the default parameters to identify various TE components in goat. To identify the position bias of TEs in the novel transcript, we searched the TEs in the 2, 000 bp upstream of TSS (Transcription Start Site) of each transcript identified in the goat genome (http://goat.kiz.ac.cn) and plotted read coverage at TSSs with the ggplot2 package in R(Wickham 2009).

Differential expression and functional enrichment analysis

Cuffdiff provides statistical routines to determine differential expression in digital transcript or gene expression data using a model based on the negative binomial distribution (Trapnell *et al.* 2010). For biological replicates, transcripts or genes with a *P*-adjust<0.05 were considered differentially expressed. To identify the molecular events or cascades involved, the differentially expressed genes or lncRNA target genes were analyzed using the DAVID platform (Huang Da *et al.* 2009b; Huang Da *et al.* 2009a). Significance was expressed as a *P*-value, which was calculated using the EASE score (a *P*-value of 0.05 was considered significant).

Validation of gene expression in RNA-seq using quantitative PCR

To validate the gene expression in RNA-seq, the total RNA from the RNA-seq analysis was used for qPCR (Fig. 4). Briefly, first strain cDNA was obtained using a One Step cDNA Synthesis Kit (Bio-Rad, USA), and the mRNA was then quantified using a standard SYBR with *GAPDH* as an endogenous control. Quantitative PCR was performed under the following conditions: 95°C for 30 sec, 40 cycles of 95°C for 5 sec, and the optimized annealing temperature for 30 sec. The primers and annealing temperatures for the 8 genes are listed in Table S1. All reactions were performed in triplicate for each sample. Gene expression was quantified relative to *GAPDH* expression using the $2^{(-\Delta Ct)}$ method. Corrections for multiple comparisons were performed using the Holm-Sidak method.

Statistical analysis

Data analyses were performed using the R statistical package.

Data availability

Figure S1 contains classification of the raw reads by RNA-seq for each of the libraries (samples) in the hyperpigmented and normal fetal goats. Figure S2 contains a heatmap of the cluster

207 analysis for the differentially expressed genes. Table S1 contains statistics of the mapping reads
208 to the reference genome. Table S2 contains annotation of novel transcripts in Swiss-Prot database.
209 Table S3 contains differential exon usage (DEU) analysis of the mRNAs in goat fetal skin. Table
210 S4 contains the differentially expressed genes between the wild-type and hyperpigmented goat
211 skins. Table S5 contains results of GO and KEGG analysis of the up-regulated DE genes using
212 DAVID. Table S6 contains results of functional annotation clustering of the DE genes using
213 DAVID.

214

215 RESULTS

216 RNA sequencing of skin in fetal goats

217 As for phenotype, there are obvious differences in skin tissue pigmentation between the two
218 breeds of fetal goat (Fig. 1A and B). Then we examined the phenotypic differences at the
219 histological level using H & E staining. The results demonstrated that there were more melanin
220 granules in the 100-day fetal epidermal and dermal layers in the Youzhou dark goat than in the
221 Yudong white goat (Fig. 1C and D). To further explore the mechanism underpinning the
222 differences in skin pigmentation, we characterized the skin transcriptome using RNA-seq
223 performed with the Illumina HiSeq 2000 platform. In the present study, we obtained a total of
224 923,013,870 raw reads from 6 libraries (samples), of which 841,895,634 clean reads remained for
225 further analysis after discarding the raw reads that contained adapter sequences, N sequences and
226 low quality sequences. The percentage of clean reads among the raw tags in each library ranged
227 from 88.39% to 93.02% (Fig. S1). We then mapped the clean reads to the goat reference genome

(http://goat.kiz.ac.cn). Of the total reads from each library, more than 83% matched to a unique genomic location, whereas only 3% matched to multiple genomic locations (Table S1). The Phred score (Q20) for each library was greater than 95.4%, which indicates our RNA-seq data were high quality and suitable for the subsequent analyses.

Novel transcripts in goat genome

We identified a total of 27,947 mRNAs and 1616 novel transcripts in fetal goat skin in the present study. To examine their homology with proteins in state-of-the-art database, we made a BLAST alignment for these novel transcripts in Swiss-Prot database (http://www.uniprot.org/). Results showed that 660 of them had a similarity in various degree, but with a relative lower coverage to the known proteins (Table S2). Another 956 novel transcripts were found without annotation in the state-of-the-art database presently. Then we examined the differences in gene length and expression levels (FPKMs) between the two groups of novel transcripts, and found that there were significant differences in gene length (Kolmogorov-Smirnov test, $P = 0.011$; Fig 2A) and expression levels (Kolmogorov-Smirnov test, $P = 0.000$; Fig 2B) between them. To further characterize the two groups of novel transcripts, we examined the composition of transposable elements (TEs) harboring in their gene sequences. Our results demonstrated that there were considerable differences in density of various TE components between the two groups of novel transcripts, as well as between the novel transcripts and mRNAs (Fig 2C). Further investigation of position bias for TEs relative to TSS (transcription start site) revealed that the LINE/RTE-BovB were higher enriched in novel transcripts without annotation than the other two groups (Fig 2D). These above findings suggest that the identified transcripts may represent different types of novel transcripts in goat genome.

Alternative splicing of the fetal skin transcriptome

To ascertain the alternative splicing (AS) events of the skin transcriptome, we examined the data from six samples using ASprofile software. Our results showed that TSSs (alternative 5' first exon, transcription start sites), TTSs (alternative 3' last exon, transcription terminal sites), and SKIPs (skipped exons) were the three most frequently observed AS events among the 12 AS subtypes in each sample (Fig. 3A). Among the over 66,000 AS events, we observed AS events in two well-known genes involved in pigmentation, *ASIP* and *TYRP1*, which were found in both goat breeds. To further examine the AS events of the differentially expressed genes between the dark- and white-skinned goat breeds, we subsequently investigated differential exon usage of the AS events using DEXSeq software. The results demonstrated that 360 AS exons belonging to 253 known and 28 unknown genes were significantly differentially expressed between the dark- and white-skinned groups (*P*-adjust<0.05) (Table S3). Importantly, we found that some AS exons belonging to well-known genes involved in pigmentation, such as *ASIP*, *DCT*, and *RAB27A*, were significantly differentially expressed between the two different skin colors (Fig. 3B). This indicates that alternative splicing may be an important mechanism by which expression and function of ASIP, DCT, and RAB27A is regulated in melanocytes.

Identification and functional clustering analysis of the differentially expressed genes

In our data, we obtained 448 differentially expressed (DE) genes (*P*-adjusted<0.05 and fold change≥1.5) using Cuffdiff between the dark- and white-skinned goats. Of the 448 DE genes, 101 genes were up-regulated and 347 were down-regulated in the dark-skinned goats compared with the white-skinned goats (Fig. 4A, Table S4, Fig. S2). Here, to elucidate the biology of skin pigmentation in goats, we specially focused on the up-regulated DE genes in the dark-skinned

goats. Gene functional classification using DAVID demonstrated that a family of keratin (KRT) was significantly enriched in the up-regulated DE genes, including *KRT-I*, *KRT81*, *KRT83*, *KRTAP13-1*, *KRTAP11-1*, and *KRTAP7-1*, which are constitutive components of skin produced by keratinocytes. Gene ontology analysis showed that the top six biological processes were *response to inorganic substance*, *response to extracellular stimulus*, *response to reactive oxygen species*, *pigmentation during development*, *pigment biosynthetic process*, and *response to cAMP* (Table S5). KEGG analysis showed that genes involved in *melanogenesis* and the *MAPK signaling pathway* were significantly enriched. These results suggest that the up-regulated genes play important roles in the dark skin phenotype of the Youzhou dark goats.

To gain a comprehensive insight of the gene expression between the two breeds, we performed Gene ontology and pathway analyses of all DE genes between the normal and dark-skinned goats using DAVID. Functional clustering analysis of all DE genes showed that 65 annotation clusters were significantly enriched, particularly *cluster 41*, which comprises 7 terms related to hyperpigmentation including *pigment biosynthetic process*, *melanin biosynthetic process*, *pigment metabolic process*, *melanin metabolic process*, *secondary metabolic process*, *melanogenesis*, and *pigmentation during development*. Regarding the pathways involved, we identified 14 significantly overrepresented pathways (Table S6) including the *melanogenesis* pathway (Fig. 4B). Selected DE genes from the RNA-seq analysis were validated using quantitative PCR (Fig. 5). These findings provide additional evidence of the underlying diversity of dermal colors in goats on the transcriptome level. Moreover, we explored the enrichment of genes involved in human pigmentation diseases using DAVID to determine whether there are diseases with similar variations in dermal colors in goats as are observed in humans. As we expected, *ASIP* and *TYRP1* were significantly enriched in one type of OMIM disease (Table 1).

296 This suggests that *ASIP* and *TYRP1* are the two likely candidate genes responsible for dermal
297 hyperpigmentation in Youzhou dark goats.

298 DISCUSSION

299 Although transcriptomic investigations on variations in skin color have been conducted in the
300 common carp (Jiang and Bikle 2014b; Wang *et al.* 2014), red tilapia (Zhu *et al.* 2016), and
301 chickens (Zhang *et al.* 2015), few studies have investigated this topic in mammals to date. We
302 first characterized the skin transcriptome in two breeds of fetal goats that feature different skin
303 colors using deep RNA-seq methods. The present study produced a large amount of data (over
304 84.2 Gb of clean reads for six samples) and more than 86% of the total reads were mapped to the
305 goat reference genome (http://goat.kiz.ac.cn), which indicated that the RNA-seq data were of
306 high quality and valuable for further analysis. First, we identified a significant number of AS
307 events (Fig. 3A) in the skin transcriptome of fetal goats, which suggests that gene transcription
308 and regulation is complex in the skin during this developmental stage in goats. AS events are
309 tissue specific and widespread in the genome (Xu *et al.* 2002). AS produces variety in the
310 proteins translated from a limited number of genes through significant alterations in protein
311 conformations that modulate cell functions (Yura *et al.* 2006). Our findings (Fig. 3; Table S3)
312 indicate that alternative splicing may be an important mechanism by which the function of ASIP,
313 *TYRP1*, *DCT*, and *RAB27A* are regulated in melanocytes. Therefore, it is necessary to identify the
314 isoforms of these genes and their roles in pigmentation in the future. Interestingly, in the present
315 study, we did not observe alternative splicing of the *MITF* gene in the skin, whereas multiple
316 splice variants of *MITF* were previously found in other species such as sheep (Saravanaperumal
317 *et al.* 2014), mice (Bismuth *et al.* 2005), and humans (Kuiper *et al.* 2004). There might be

differences in the regulatory mechanisms of skin pigmentation between goats and the species mentioned above. Another valuable finding of the present study is the DE genes identified in the fetal skin between the two goat groups. In particular, members of the keratin family were highly differentially expressed in the fetal skin between the two goat groups, including *KRT1*, *KRT81*, *KRT83*, *KRTAP13-1*, *KRTAP11-1*, and *KRTAP7-1* (Table S5). Keratins make up the largest subgroup of intermediate filament proteins and represent the most abundant proteins in epithelial cells. These proteins are essential to sustain normal epidermal function and play a role in signaling (Porter and Lane 2003). Mutations of a member of the KRT family resulted in an unusual skin pigmentation in humans (Irvine *et al.* 1997; Horiguchi *et al.* 2005; Pascucci *et al.* 2006; Geller *et al.* 2013). Therefore, these DE keratins might participate in the signaling transduction involved in melanin synthesis in melanocytes or the transportation of melanin from melanocytes to keratinocytes through cellular interactions (Nakazawa *et al.* 1995; Seiberg 2001; Joshi *et al.* 2007).

Further functional clustering analysis of the DE genes showed that the terms involved in pigmentation and melanogenesis were highly overrepresented in our findings (Table S5 and S6), which is similar to the findings from studies on coat color in sheep (Fan *et al.* 2013) and skin color in the common carp (Jiang and Bikle 2014a). However, the specific DE genes of the skin differed in this study compared with the studies above. Specifically, the melanogenic *ASIP* (fold change >31) and *TYRP1* (fold change >87) were not only among the most significantly DE genes between the dark- and white-skinned goats, but were also associated with human pigmentation (Table 1). Previous studies have demonstrated that polymorphisms of *ASIP* are associated with darker skin color in African Americans (Bonilla *et al.* 2005) and fair skin color in Caucasians (Nan *et al.* 2009). *TYRP1*, a key regulator of melanin biosynthesis in melanocytes, is reported to

be involved in the diversity of skin color in Europeans (Lao *et al.* 2007) and is a candidate gene for skin color (such as mouth, nose, and ear) in sheep (Raadsma *et al.* 2013). In addition, *DCT* is also associated with variations of skin pigmentation in Asians (Myles *et al.* 2007). However, the results of the present study suggest that *ASIP* is more likely the candidate gene for skin color in goats than *TYRP1* and *DCT*. We believe that *TYRP1* and *DCT* are two downstream genes whose expression levels are affected by *ASIP* in the KEGG pathway *melanogenesis* (Fig. 4B). However, efforts still be taken to ascertain the candidate genes underlying variations of skin color in goats using gene mapping techniques such as genome wide association studies (GWAS), next generation sequencing (NGS), or quantitative trait loci (QTL) analyses.

Our another valuable finding is the novel transcripts identified by RNA-seq (Table S1). Cabili, *et al* (2011) characterized a class of novel transcripts that were excluded by their coding potential criteria (a Pfam domain, a positive PhyloCSF score, or previously annotated as pseudogenes), and firstly termed them as TUCP (transcripts of uncertain coding potential) (Cabili *et al.* 2011). Since they merely focused the lincRNAs in human genome under a certain classification strategy, other subtypes of lncRNAs such as intronic lncRNAs and antisense lncRNAs were retained and thus grouped into the catalog of TUCP in their findings. However, in the present study, the intronic lncRNAs and antisense lncRNAs were absolutely excluded from the novel transcripts based on our recent study (Ren *et al.* 2016). Thus there are certain differences in classification of novel transcripts between the study from Cabili *et al* and ours. In view of subsequent analyses, we are certain that the identified transcripts with annotation and without annotation are two different groups of novel transcripts. Especially for those without annotation, the characteristics of a relatively low expression level and a highly enrichment of TE component (LINE/RTE-BovB) around TSS (transcription start site) (Fig 2) which are similar with that of the lincRNAs in recent

364 studies (Cabili *et al.* 2011; Derrien *et al.* 2012; Kelley and Rinn 2012; Li *et al.* 2012; Nam and
365 Bartel 2012; Billerey *et al.* 2014; Ren *et al.* 2016), strongly suggest this group of novel
366 transcripts could be long nocoding RNAs. However, we are not certain that the novel transcripts
367 with some annotation should be protein coding genes or long nocoding RNAs based on the
368 current knowledge. It still need further efforts to identify their identity. Generally, this study
369 provides a valuable resource for the genetic mechanisms involved in pigmentation diseases and
370 contributes to the understanding of the biology of skin pigmentation and development in
371 mammals.

372

373 ACKNOWLEDGEMENTS

374 We thank Dr. Sun Wu, Sun Xiaowei, and their colleages from Southwest University for assistance
375 in the sampling and experiments. We also thank Ms Yuan Jingxian and her colleagues for data
376 processing in Novogene LTD. Co (Beijing). This work was supported by grants from the
377 Chongqing Fund of application and development (cstc2013yykfC80003), the Chongqing
378 Fundamental Research Funds (2013cstc-jbky-00106-zj; No.15435), and the Chongqing Fund of
379 Agriculture Development (No.14412, No.15404).

380 LITERATURE CITED

381 Anders, S., A. Reyes and W. Huber, 2012 Detecting differential usage of exons from RNA-seq data. Genome Res 22:
382 2008-2017.
383 Baxter, L. L., and W. J. Pavan, The etiology and molecular genetics of human pigmentation disorders. Wiley
384 Interdiscip Rev Dev Biol 2: 379-392.
385 Bennett, D. C., and M. L. Lamoreux, 2003 The color loci of mice--a genetic century. Pigment Cell Res 16: 333-344.
386 Billerey, C., M. Boussaha, D. Esquerre, E. Rebours, A. Djari *et al.*, 2014 Identification of large intergenic non-coding
387 RNAs in bovine muscle using next-generation transcriptomic sequencing. BMC Genomics 15: 499.
388 Bismuth, K., D. Maric and H. Arnheiter, 2005 MITF and cell proliferation: the role of alternative splice forms. Pigment
389 Cell Res 18: 349-359.

Bonilla, C., L. A. Boxill, S. A. Donald, T. Williams, N. Sylvester *et al.*, 2005 The 8818G allele of the agouti signaling protein (ASIP) gene is ancestral and is associated with darker skin color in African Americans. Hum Genet 116: 402-406.

Cabili, M. N., C. Trapnell, L. Goff, M. Koziol, B. Tazon-Vega *et al.*, 2011 Integrative annotation of human large intergenic noncoding RNAs reveals global properties and specific subclasses. Genes Dev 25: 1915-1927.

Derrien, T., R. Johnson, G. Bussotti, A. Tanzer, S. Djebali *et al.*, 2012 The GENCODE v7 catalog of human long noncoding RNAs: analysis of their gene structure, evolution, and expression. Genome Res 22: 1775-1789.

Dorshorst, B., A. M. Molin, C. J. Rubin, A. M. Johansson, L. Stromstedt *et al.*, 2011 A complex genomic rearrangement involving the endothelin 3 locus causes dermal hyperpigmentation in the chicken. PLoS Genet 7: e1002412.

Ebanks, J. P., R. R. Wickett and R. E. Boissy, 2009 Mechanisms regulating skin pigmentation: the rise and fall of complexion coloration. Int J Mol Sci 10: 4066-4087.

Fan, R., J. Xie, J. Bai, H. Wang, X. Tian *et al.*, 2013 Skin transcriptome profiles associated with coat color in sheep. BMC Genomics 14: 389.

Florea, L., L. Song and S. L. Salzberg, 2013 Thousands of exon skipping events differentiate among splicing patterns in sixteen human tissues. F1000Res 2: 188.

Gao, Y., X. Wang, H. Yan, J. Zeng, S. Ma *et al.*, 2016 Comparative Transcriptome Analysis of Fetal Skin Reveals Key Genes Related to Hair Follicle Morphogenesis in Cashmere Goats. PLoS One 11: e0151118.

Garcia-Gamez, E., A. Reverter, V. Whan, S. M. McWilliam, J. J. Arranz *et al.*, 2011 Using regulatory and epistatic networks to extend the findings of a genome scan: identifying the gene drivers of pigmentation in merino sheep. PLoS One 6: e21158.

Garcia, S., F. Diaz and C. T. Moraes, 2008 A 3' UTR modification of the mitochondrial rieske iron sulfur protein in mice produces a specific skin pigmentation phenotype. J Invest Dermatol 128: 2343-2345.

Geller, L., L. Kristal and K. D. Morel, 2013 Epidermolysis bullosa simplex with mottled pigmentation due to a rare keratin 5 mutation: cutaneous findings in infancy. Pediatr Dermatol 30: 631-632.

Guttman, M., M. Garber, J. Z. Levin, J. Donaghey, J. Robinson *et al.*, 2010 Ab initio reconstruction of cell type-specific transcriptomes in mouse reveals the conserved multi-exonic structure of lincRNAs. Nat Biotechnol 28: 503-510.

Han, J. L., M. Yang, Y. J. Yue, T. T. Guo, J. B. Liu *et al.*, 2015 Analysis of agouti signaling protein (ASIP) gene polymorphisms and association with coat color in Tibetan sheep (Ovis aries). Genet Mol Res 14: 1200-1209.

Horiguchi, Y., D. Sawamura, R. Mori, H. Nakamura, K. Takahashi *et al.*, 2005 Clinical heterogeneity of 1649delG mutation in the tail domain of keratin 5: a Japanese family with epidermolysis bullosa simplex with mottled pigmentation. J Invest Dermatol 125: 83-85.

Huang da, W., B. T. Sherman and R. A. Lempicki, 2009a Bioinformatics enrichment tools: paths toward the comprehensive functional analysis of large gene lists. Nucleic Acids Res 37: 1-13.

Huang da, W., B. T. Sherman and R. A. Lempicki, 2009b Systematic and integrative analysis of large gene lists using DAVID bioinformatics resources. Nat Protoc 4: 44-57.

Irvine, A. D., K. E. McKenna, H. Jenkinson and A. E. Hughes, 1997 A mutation in the V1 domain of keratin 5 causes epidermolysis bullosa simplex with mottled pigmentation. J Invest Dermatol 108: 809-810.

Jiang, Y. J., and D. D. Bikle, 2014a LncRNA profiling reveals new mechanism for VDR protection against skin cancer formation. J Steroid Biochem Mol Biol 144 Pt A: 87-90.

Jiang, Y. J., and D. D. Bikle, 2014b LncRNA: a new player in 1alpha, 25(OH)(2) vitamin D(3) /VDR protection against skin cancer formation. Exp Dermatol 23: 147-150.

Joshi, P. G., N. Nair, G. Begum, N. B. Joshi, V. P. Sinkar *et al.*, 2007 Melanocyte-keratinocyte interaction induces calcium signalling and melanin transfer to keratinocytes. Pigment Cell Res 20: 380-384.

Kelley, D., and J. Rinn, 2012 Transposable elements reveal a stem cell-specific class of long noncoding RNAs. Genome Biol 13: R107.

Kim, D., G. Pertea, C. Trapnell, H. Pimentel, R. Kelley *et al.*, 2013 TopHat2: accurate alignment of transcriptomes in the presence of insertions, deletions and gene fusions. Genome Biol 14: R36.

Kondo, T., and V. J. Hearing, 2011 Update on the regulation of mammalian melanocyte function and skin pigmentation. Expert Rev Dermatol 6: 97-108.

Kong, L., Y. Zhang, Z. Q. Ye, X. Q. Liu, S. Q. Zhao *et al.*, 2007 CPC: assess the protein-coding potential of transcripts

using sequence features and support vector machine. Nucleic Acids Res 35: W345-349.

Kuiper, R. P., M. Schepens, J. Thijssen, E. F. Schoenmakers and A. G. van Kessel, 2004 Regulation of the MiTF/TFE bHLH-LZ transcription factors through restricted spatial expression and alternative splicing of functional domains. Nucleic Acids Res 32: 2315-2322.

Langmead, B., and S. L. Salzberg, 2012 Fast gapped-read alignment with Bowtie 2. Nat Methods 9: 357-359.

Langmead, B., C. Trapnell, M. Pop and S. L. Salzberg, 2009 Ultrafast and memory-efficient alignment of short DNA sequences to the human genome. Genome Biol 10: R25.

Lao, O., J. M. de Gruijter, K. van Duijn, A. Navarro and M. Kayser, 2007 Signatures of positive selection in genes associated with human skin pigmentation as revealed from analyses of single nucleotide polymorphisms. Ann Hum Genet 71: 354-369.

Lee, S., D. H. Kim, G. Lee, K. U. Whang, J. S. Lee *et al.*, 2010 An unusual case of congenital dermal melanocytosis. Ann Dermatol 22: 460-462.

Li, T., S. Wang, R. Wu, X. Zhou, D. Zhu *et al.*, 2012 Identification of long non-protein coding RNAs in chicken skeletal muscle using next generation sequencing. Genomics 99: 292-298.

Lin, M. F., I. Jungreis and M. Kellis, 2011 PhyloCSF: a comparative genomics method to distinguish protein coding and non-coding regions. Bioinformatics 27: i275-282.

Liu, F., B. Wen and M. Kayser, 2013 Colorful DNA polymorphisms in humans. Semin Cell Dev Biol 24: 562-575.

Meng, S., M. Zhang, L. Liang and J. Han, 2012 Current opportunities and challenges: genome-wide association studies on pigmentation and skin cancer. Pigment Cell Melanoma Res 25: 612-617.

Muroya, S., R. Tanabe, I. Nakajima and K. Chikuni, 2000 Molecular characteristics and site specific distribution of the pigment of the silky fowl. J Vet Med Sci 62: 391-395.

Myles, S., M. Somel, K. Tang, J. Kelso and M. Stoneking, 2007 Identifying genes underlying skin pigmentation differences among human populations. Hum Genet 120: 613-621.

Nakazawa, K., H. Nakazawa, C. Collombel and O. Damour, 1995 Keratinocyte extracellular matrix-mediated regulation of normal human melanocyte functions. Pigment Cell Res 8: 10-18.

Nam, J. W., and D. P. Bartel, 2012 Long noncoding RNAs in C. elegans. Genome Res 22: 2529-2540.

Nan, H., P. Kraft, D. J. Hunter and J. Han, 2009 Genetic variants in pigmentation genes, pigmentary phenotypes, and risk of skin cancer in Caucasians. Int J Cancer 125: 909-917.

Nozaki, A., and T. Makita, 1998 The surface color measurement of major tissues of silky fowls and White Leghorns. J Vet Med Sci 60: 489-493.

Pascucci, M., P. Posteraro, C. Pedicelli, A. Provini, L. Auricchio *et al.*, 2006 Epidermolysis bullosa simplex with mottled pigmentation due to de novo P25L mutation in keratin 5 in an Italian patient. Eur J Dermatol 16: 620-622.

Porter, R. M., and E. B. Lane, 2003 Phenotypes, genotypes and their contribution to understanding keratin function. Trends Genet 19: 278-285.

Punta, M., P. C. Coggill, R. Y. Eberhardt, J. Mistry, J. Tate *et al.*, 2012 The Pfam protein families database. Nucleic Acids Res 40: D290-301.

Qin, P., 2001 *Embryology in Mammals*. Science Press, Beijing.

Quillen, E. E., and M. D. Shriver, 2011 Unpacking human evolution to find the genetic determinants of human skin pigmentation. J Invest Dermatol 131: E5-7.

Raadsma, H. W., E. Jonas, M. R. Fleet, K. Fullard, J. Gongora *et al.*, 2013 QTL and association analysis for skin and fibre pigmentation in sheep provides evidence of a major causative mutation and epistatic effects. Anim Genet 44: 547-559.

Ren, H., G. Wang, L. Chen, J. Jiang, L. Liu *et al.*, 2016 Genome-wide analysis of long non-coding RNAs at early stage of skin pigmentation in goats (Capra hircus). BMC Genomics 17: 67.

Saravanaperumal, S. A., D. Pediconi, C. Renieri and A. La Terza, 2014 Alternative splicing of the sheep MITF gene: novel transcripts detectable in skin. Gene 552: 165-175.

Seiberg, M., 2001 Keratinocyte-melanocyte interactions during melanosome transfer. Pigment Cell Res 14: 236-242.

Shinomiya, A., Y. Kayashima, K. Kinoshita, M. Mizutani, T. Namikawa *et al.*, 2012 Gene duplication of endothelin 3 is closely correlated with the hyperpigmentation of the internal organs (Fibromelanosis) in silky chickens. Genetics 190: 627-638.

Slominski, A., D. J. Tobin, S. Shibahara and J. Wortsman, 2004 Melanin pigmentation in mammalian skin and its hormonal regulation. Physiol Rev 84: 1155-1228.

Sturm, R. A., 2009 Molecular genetics of human pigmentation diversity. Hum Mol Genet 18: R9-17.

Sun, L., H. Luo, D. Bu, G. Zhao, K. Yu *et al.*, 2013 Utilizing sequence intrinsic composition to classify protein-coding and long non-coding transcripts. Nucleic Acids Res 41: e166.

Trapnell, C., A. Roberts, L. Goff, G. Pertea, D. Kim *et al.*, 2012 Differential gene and transcript expression analysis of RNA-seq experiments with TopHat and Cufflinks. Nat Protoc 7: 562-578.

Trapnell, C., B. A. Williams, G. Pertea, A. Mortazavi, G. Kwan *et al.*, 2010 Transcript assembly and quantification by RNA-Seq reveals unannotated transcripts and isoform switching during cell differentiation. Nat Biotechnol 28: 511-515.

Wang, C., M. Wachholtz, J. Wang, X. Liao and G. Lu, 2014 Analysis of the skin transcriptome in two oujiang color varieties of common carp. PLoS One 9: e90074.

Wang, L., L. Peng, W. Zhang, Z. Zhang, W. Yang *et al.*, 1996 Initiation and development of skin follicles in the inner Mongolian Cashmere goat. Acta Veterinaria et Zootechnica Sinica 27: 524-530.

Wang, L., Y. Zhang, M. Zhao, R. Wang, R. Su *et al.*, 2015 SNP Discovery from Transcriptome of Cashmere Goat Skin. Asian-Australas J Anim Sci 28: 1235-1243.

Weikard, R., F. Hadlich and C. Kuehn, 2013 Identification of novel transcripts and noncoding RNAs in bovine skin by deep next generation sequencing. BMC Genomics 14: 789.

Wickham, H., 2009 *Elegant graphics for data analysis*. Springer, New York.

Wolff, K., 1973 Melanocyte-keratinocyte interactions in vivo: the fate of melanosomes. Yale J Biol Med 46: 384-396.

Xu, Q., B. Modrek and C. Lee, 2002 Genome-wide detection of tissue-specific alternative splicing in the human transcriptome. Nucleic Acids Res 30: 3754-3766.

Xu, T., X. Guo, H. Wang, X. Du, X. Gao *et al.*, 2013a De Novo Transcriptome Assembly and Differential Gene Expression Profiling of Three Capra hircus Skin Types during Anagen of the Hair Growth Cycle. Int J Genomics 2013: 269191.

Xu, T., X. Guo, H. Wang, F. Hao, X. Du *et al.*, 2013b Differential gene expression analysis between anagen and telogen of Capra hircus skin based on the de novo assembled transcriptome sequence. Gene 520: 30-38.

Yamaguchi, Y., M. Brenner and V. J. Hearing, 2007 The regulation of skin pigmentation. J Biol Chem 282: 27557-27561.

Yamaguchi, Y., and V. J. Hearing, 2009 Physiological factors that regulate skin pigmentation. Biofactors 35: 193-199.

Yue, Y. J., J. B. Liu, M. Yang, J. L. Han, T. T. Guo *et al.*, 2015 De novo assembly and characterization of skin transcriptome using RNAseq in sheep (Ovis aries). Genet Mol Res 14: 1371-1384.

Yura, K., M. Shionyu, K. Hagino, A. Hijikata, Y. Hirashima *et al.*, 2006 Alternative splicing in human transcriptome: functional and structural influence on proteins. Gene 380: 63-71.

Zhang, J., F. Liu, J. Cao and X. Liu, 2015 Skin transcriptome profiles associated with skin color in chickens. PLoS One 10: e0127301.

Zhu, W., L. Wang, Z. Dong, X. Chen, F. Song *et al.*, 2016 Comparative Transcriptome Analysis Identifies Candidate Genes Related to Skin Color Differentiation in Red Tilapia. Sci Rep 6: 31347.

Figure legends

Fig. 1 Histomorphological examination of the hyperpigmented and normal skin in fetal goats.

To explore the histomorphological differences between the two breeds of goats at the early stage of skin pigmentation and development, the 100-day-old fetal skin from the Youzhou dark goat (A

538 and C) and Yudong white goat (B and D) were examined using H & E staining. The scale bar for
539 the images in (C) and (D) is 10 μm.

540 **Fig.2 Characteristic differences between two groups of novel transcripts in goat genome**

541 The transcript length (A) and expression level (B) of two classes of novel transcripts were
542 compared using the Kolmogorov-Smirnov test, and a P value of 0.05 indicates significance
543 between two groups. In two box plots, the circle indicates the outlier, and the asterisk labels the
544 extreme. (C) The proportion of the main TE families in two groups of novel transcripts and
545 mRNAs in the goat genome (http://goat.kiz.ac.cn). Differences in TE components between them
546 were measured by using the Fisher Exact test. (D) The position bias of TE components in the
547 2,000 bp upstream of TSS in transcripts above mentioned.

548 **Fig. 3 Alternative splicing (AS) events in the goat genome.**

549 Following the analysis using Cufflinks, the classification of AS events of transcripts were
550 performed for each library (sample) using the ASprofile tool. The 12 main AS events (TSS, TTS,
551 SKIP, XSKIP, MSKIP, XMSKIP, IR, XIR, MIR, XMIR, AE, and XAE) in the goat genome are
552 summarized in (A). Y1, Y2, and Y3 indicate the dark skin goats, whereas B1, B2, and B3 indicate
553 the white skin goats. (B) Differential exon usage of the AS events in the *ASIP* and *DCT* genes
554 between the dark-skinned (Y, blue) and white-skinned (B, red) goats.

555 **Fig. 4 The differentially expressed genes between the dark- and white-skinned goats.**

556 (A) The differential expression of genes was identified based on the FPKM values (corrected
557 *P*-value≤0.05 and fold change≥1.5) in the two groups. The volcano plot was generated based on
558 the values above. Y indicates the dark-skinned goats, and B refers to the white-skinned goats. (B)
559 Enrichment of the DE genes was conducted under KEGG pathways. Red indicates the

560 up-regulated DE genes and green refers to the down-regulated genes in the dark-skinned goats
561 compared to the control goats (white-skinned).

562 **Fig. 5 Validation of gene expression in the dark- and white-skinned goats using qPCR.**

563 Some of the identified melanogenic genes were examined in the dark- and white-skinned fetal
564 goats using qPCR. Gene expression was quantified relative to *GAPDH* expression using the $2^{(-\Delta Ct)}$
565 method. Corrections for multiple comparisons were performed using the Holm-Sidak method.
566 The data are shown as the mean ± 1 SE (n = 3). **P*<0.05, ***P*<0.01.

567 Additional files

568 Fig. S1. Classification of the raw reads by RNA-seq for each of the libraries (samples) in the
569 hyperpigmented and normal fetal goats.

570 Fig. S2. Heatmap of the cluster analysis for the differentially expressed genes.

571 Table S1. Statistics of the mapping reads to the reference genome.

572 Table S2. Annotation of novel transcripts in Swiss-Prot database.

573 Table S3. Differential exon usage (DEU) analysis of the mRNAs in goat fetal skin.

574 Table S4. Differentially expressed genes between the wild-type and hyperpigmented goat skins.

575 Table S5. GO and KEGG analysis of the up-regulated DE genes using DAVID.

576 Table S6. Functional annotation clustering of the DE genes using DAVID.

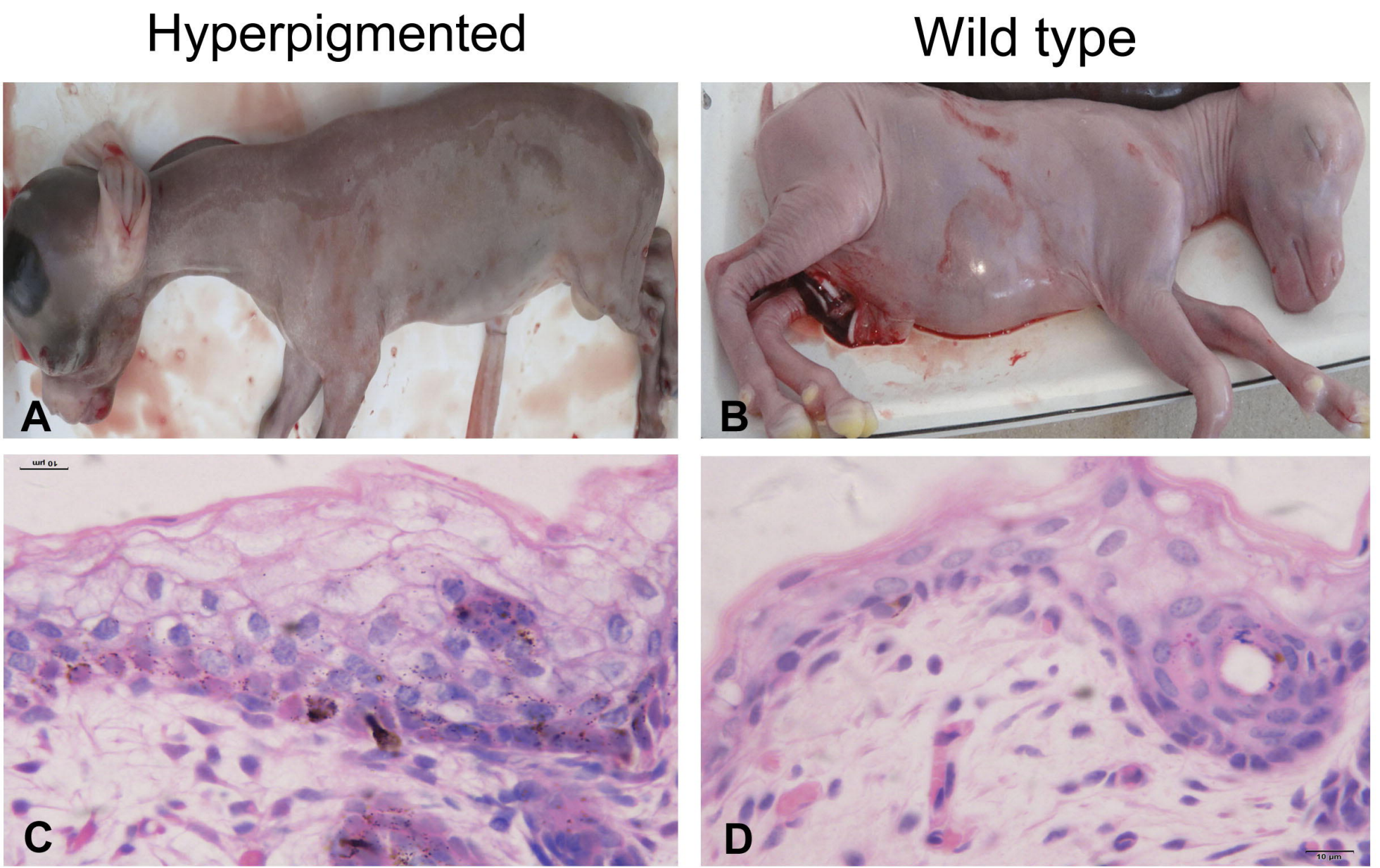
Hyperpigmented
Wild type
A
B
C
D
10 µm

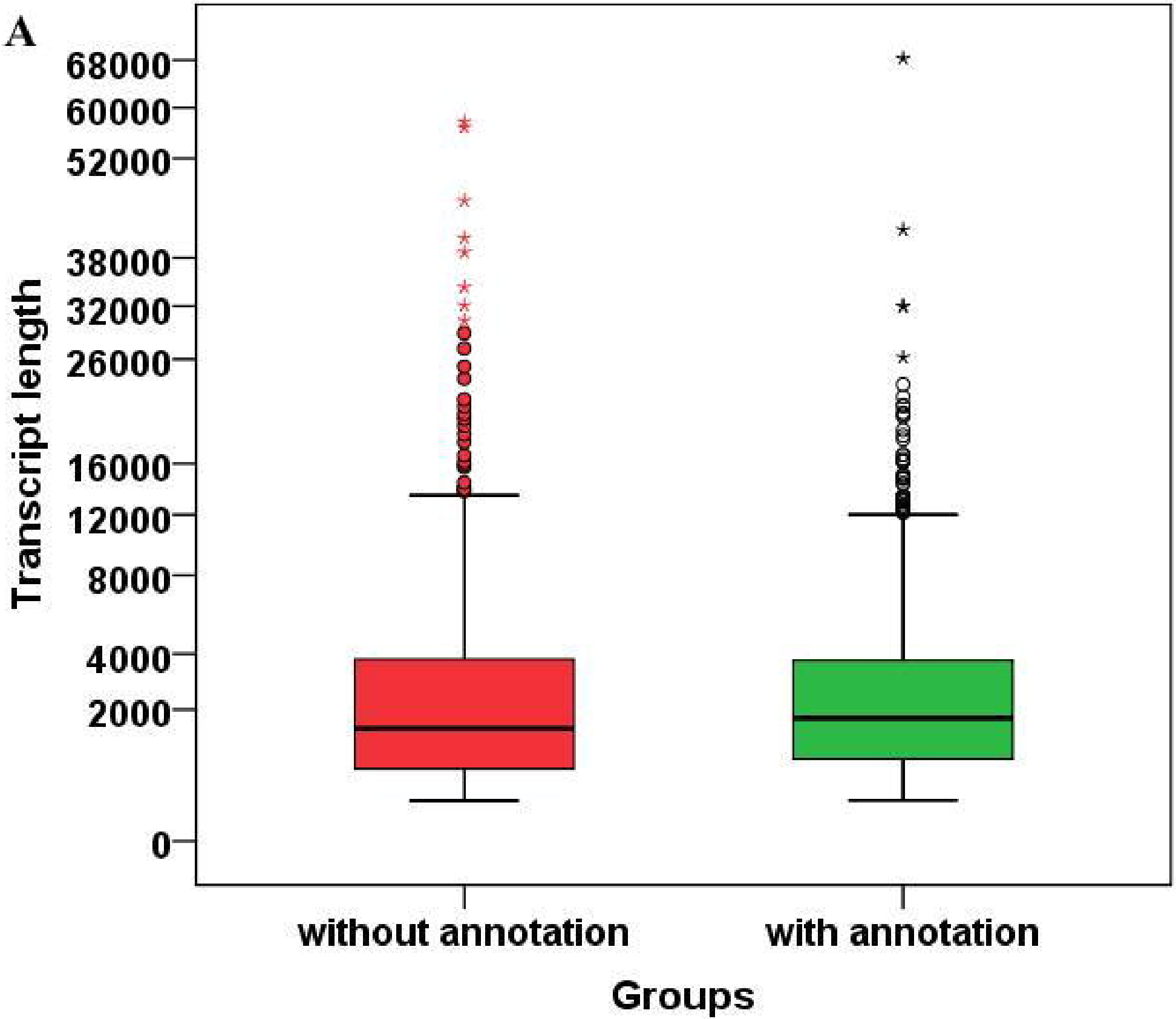
A
68000
60000
52000
38000
32000
26000
16000
12000
8000
4000
2000
0
Transcript length
without annotation
with annotation
Groups

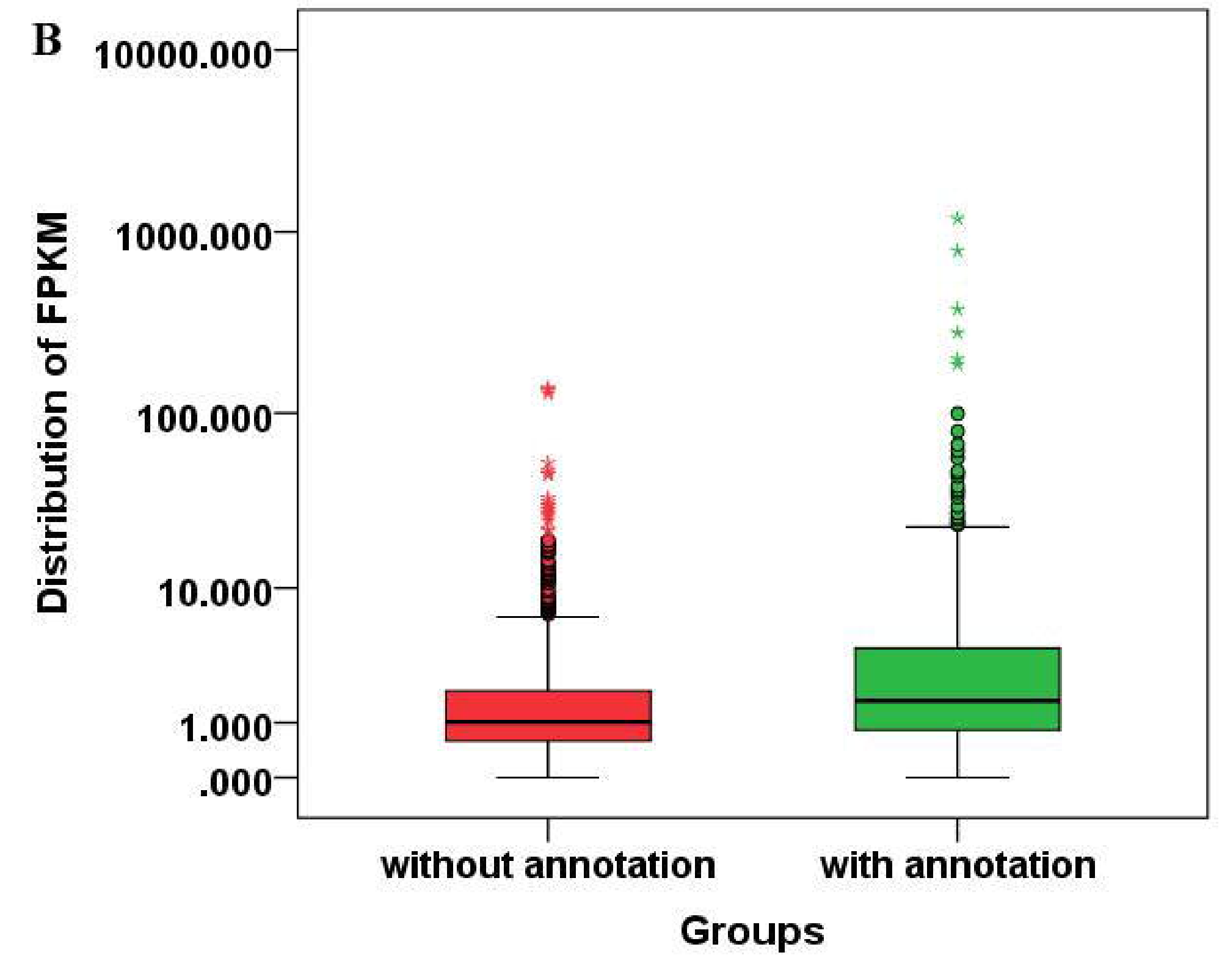
B
10000.000
1000.000
100.000
10.000
1.000
.000
Distribution of FPKM
without annotation
with annotation
Groups

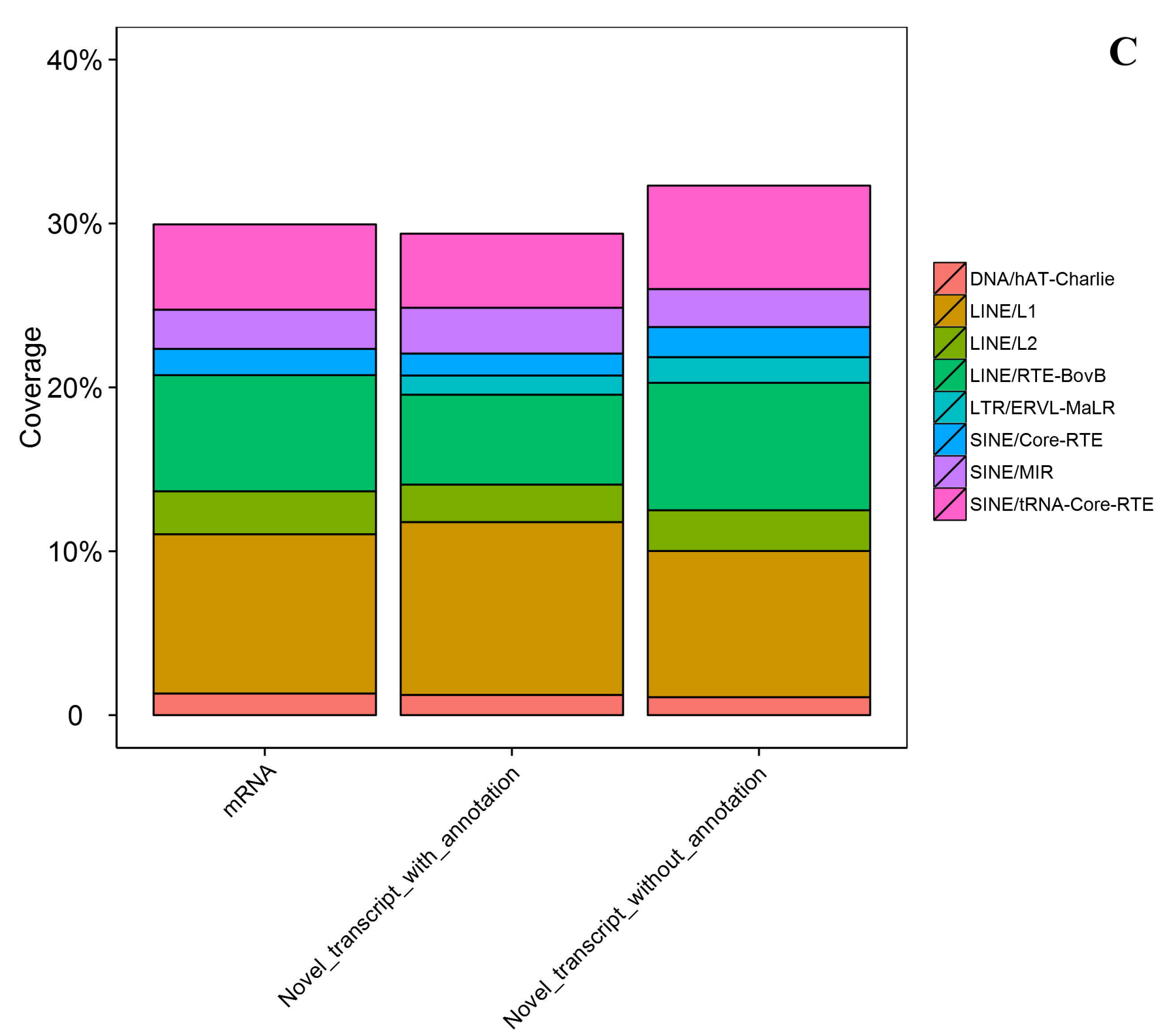
C
40%
30%
20%
10%
0
Coverage
mRNA
Novel_transcript_with_annotation
Novel_transcript_without_annotation
DNA/hAT-Charlie
LINE/L1
LINE/L2
LINE/RTE-BovB
LTR/ERVL-MaLR
SINE/Core-RTE
SINE/MIR
SINE/tRNA-Core-RTE

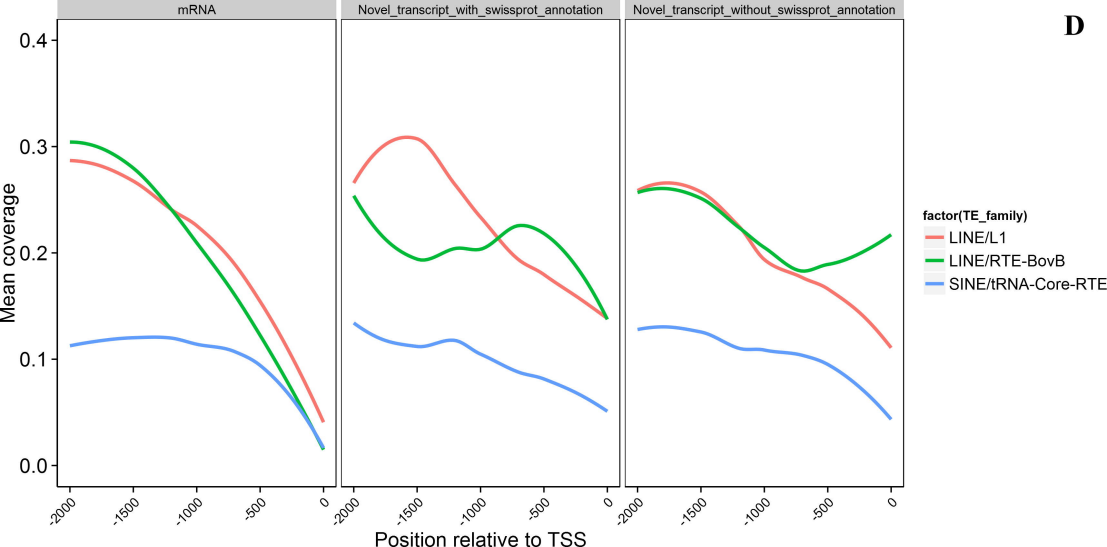
D
mRNA
Novel_transcript_with_swissprot_annotation
Novel_transcript_without_swissprot_annotation
Mean coverage
0.4
0.3
0.2
0.1
0.0
-2000
-1500
-1000
-500
0
Position relative to TSS
factor(TE_family)
LINE/L1
LINE/RTE-BovB
SINE/tRNA-Core-RTE

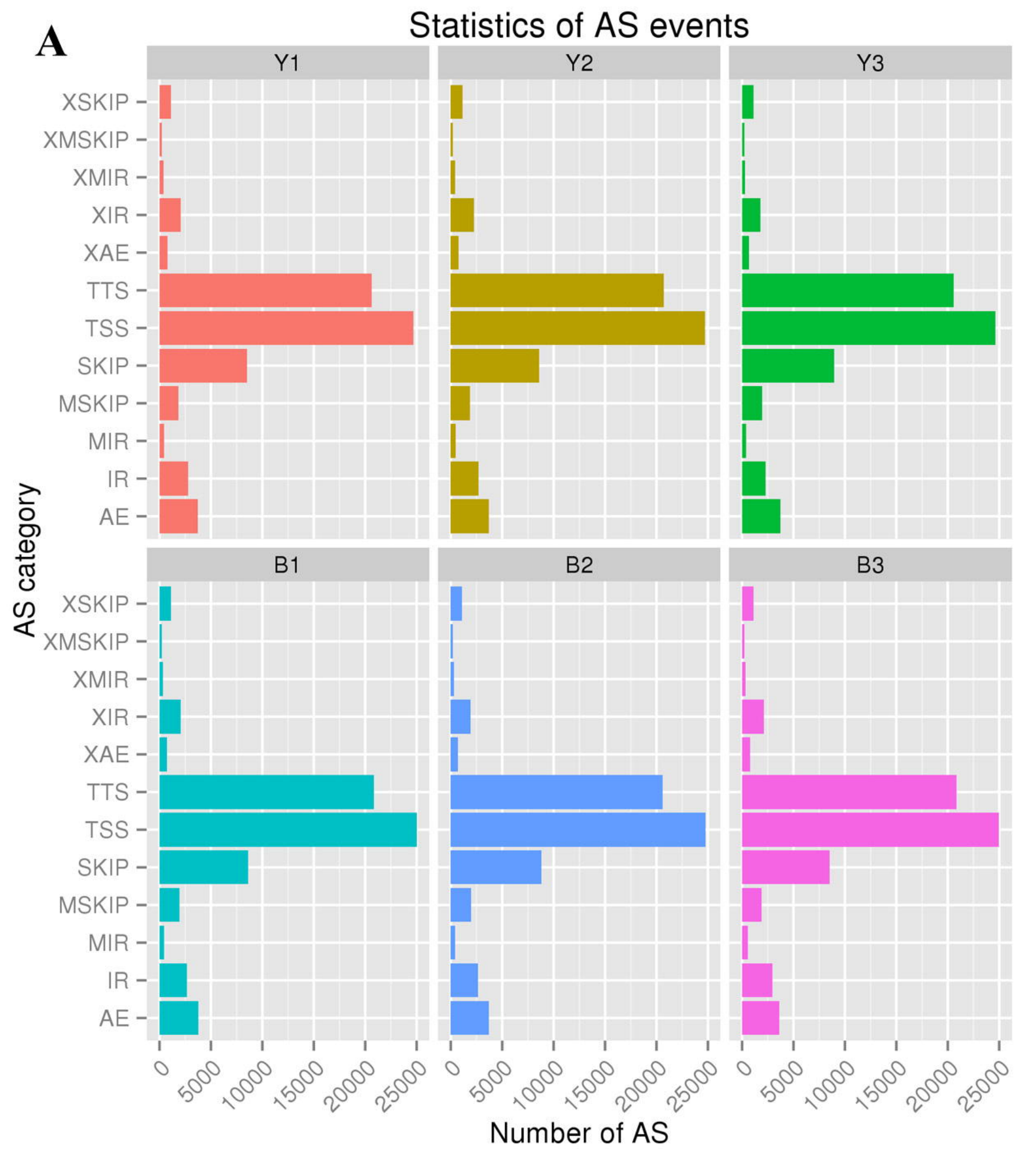
A
Statistics of AS events
Y1
Y2
Y3
B1
B2
B3
XSKIP
XMSKIP
XMIR
XIR
XAE
TTS
TSS
SKIP
MSKIP
MIR
IR
AE
AS category
0
5000
10000
15000
20000
25000
Number of AS

B

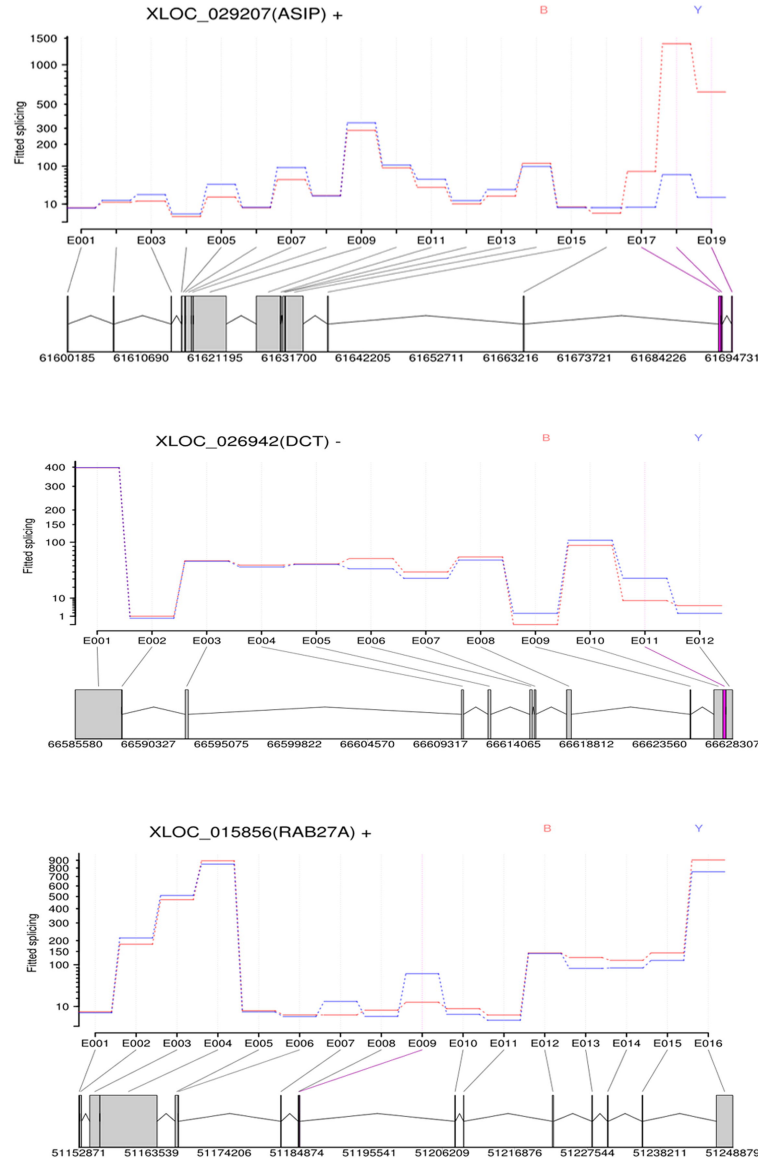
XLOC_029207(ASIP) +
B
Y
Fitted splicing
1500
1000
500
300
200
100
10
E001
E003
E005
E007
E009
E011
E013
E015
E017
E019
61600185
61610690
61621195
61631700
61642205
61652711
61663216
61673721
61684226
61694731
XLOC_026942(DCT) -
B
Y
Fitted splicing
400
300
200
150
100
10
1
E001
E002
E003
E004
E005
E006
E007
E008
E009
E010
E011
E012
66585580
66590327
66595075
66599822
66604570
66609317
66614065
66618812
66623560
66628307
XLOC_015856(RAB27A) +
B
Y
Fitted splicing
900
800
700
600
500
400
300
200
150
100
10
E001
E002
E003
E004
E005
E006
E007
E008
E009
E010
E011
E012
E013
E014
E015
E016
51152871
51163539
51174206
51184874
51195541
51206209
51216876
51227544
51238211
51248879

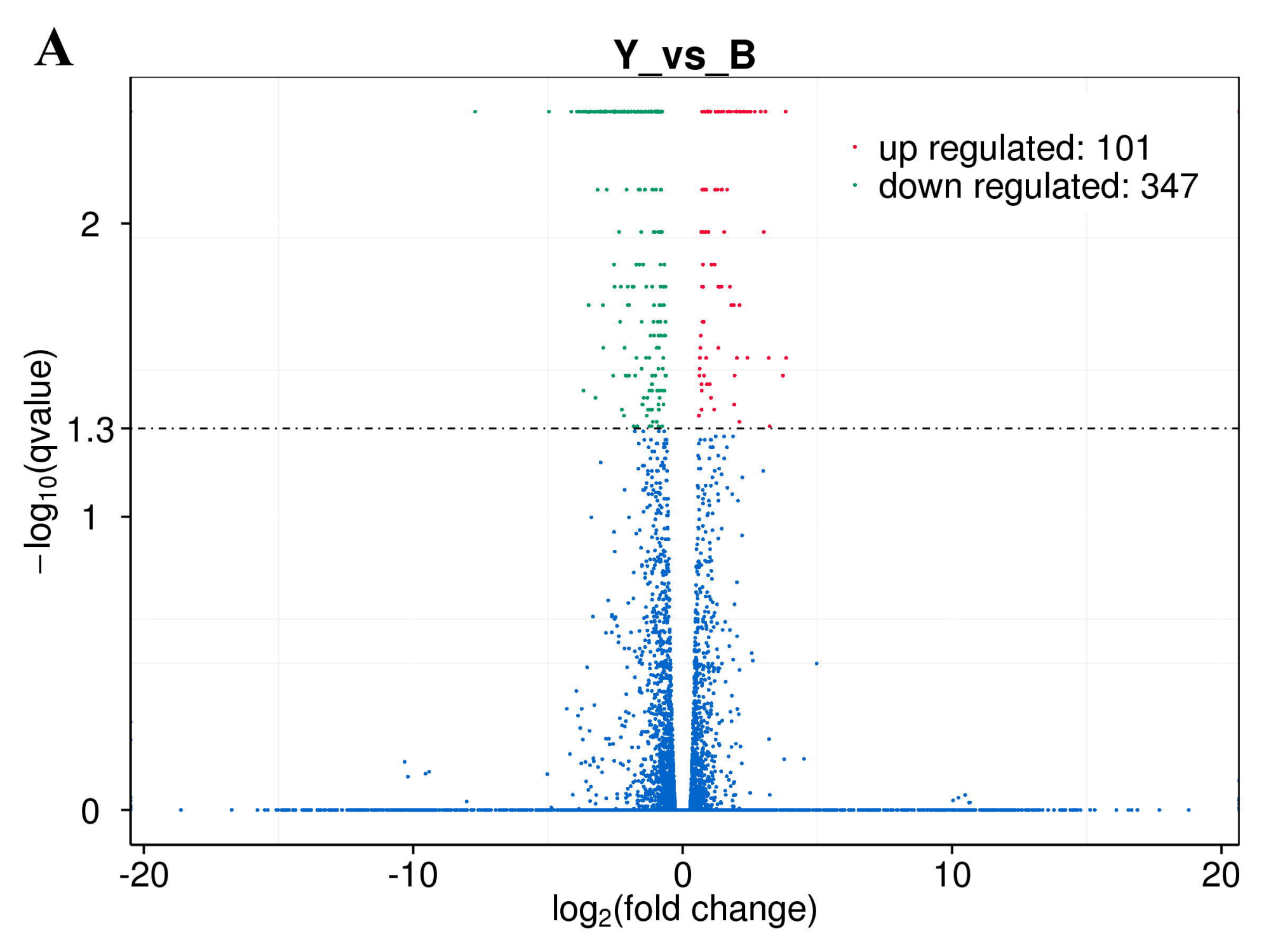
A
Y_vs_B
up regulated: 101
down regulated: 347
2
1.3
1
0
−log10(qvalue)
-20
-10
0
10
20
log2(fold change)

B

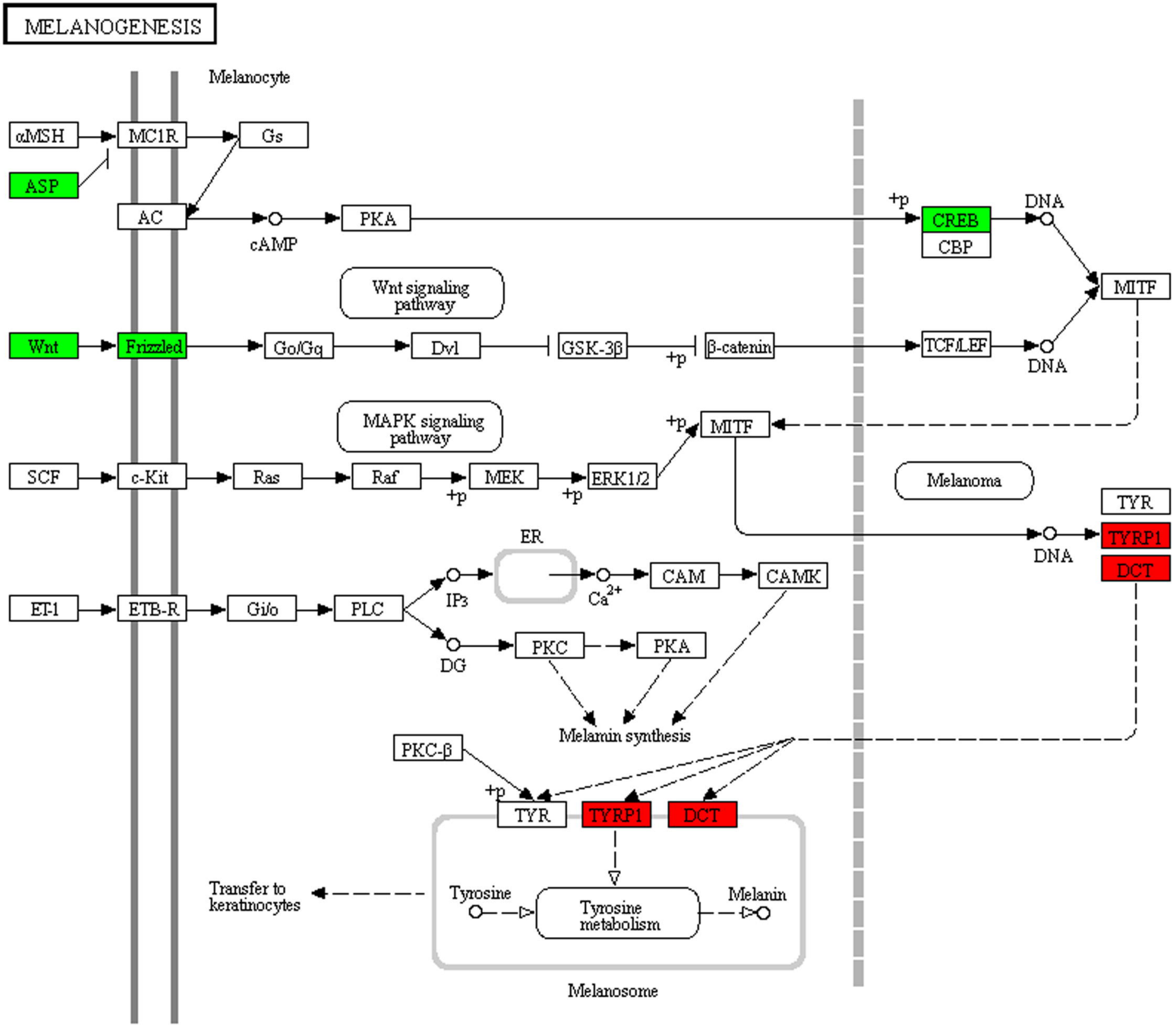

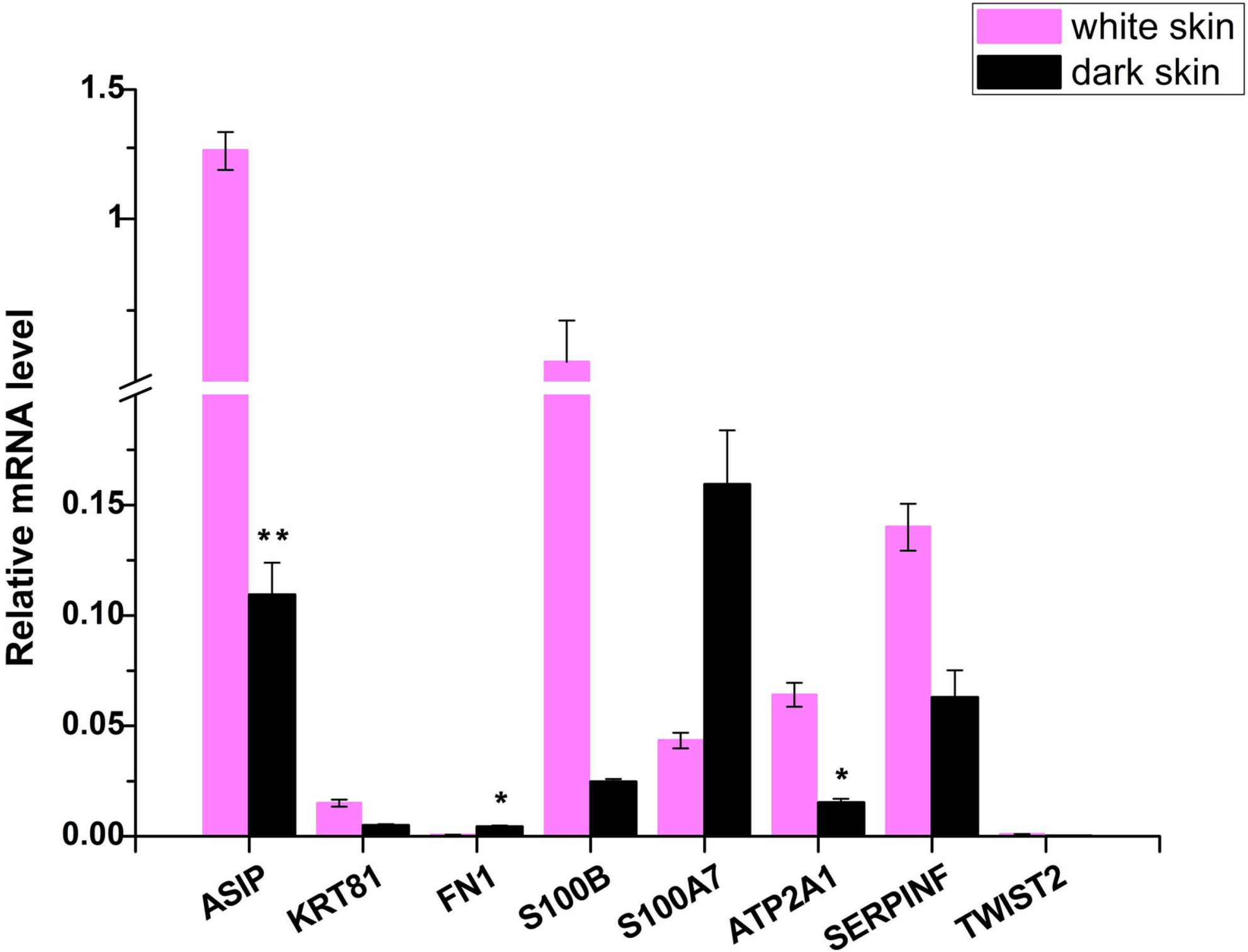
white skin
dark skin
Relative mRNA level
1.5
1
0.15
0.10
0.05
0.00
**
*
*
ASIP
KRT81
FN1
S100B
S100A7
ATP2A1
SERPINF
TWIST2